1

Organic Heterostructure in Electronic Devices

1.1 Organic Light-Emitting Diodes

In 1987, C.W. Tang was the first to report organic light-emitting diodes with a double layer structure [1]. Light emission can be observed at about 2.5 V, and a high brightness (> 1000 cd/m^2) is achievable at a driving voltage < 10 V. The mechanism was explained by a model of separate carrier transport layers. The electron transport layer (ETL) and the hole transport layer (HTL) are equivalent to n- and p-type semiconductors. The electrons and holes are injected into electron and hole transport layers from cathode Au and anode indium tin oxide (ITO), respectively, and the radiative recombination of injected electrons and holes then takes place in the Alq_3 layer (Figure 1.1).

In 1990, scientists in Cambridge University also produced electroluminescence by using a conjugate polymer heterostructure, usually called polymer light-emitting diodes (PLEDs) [2]. Organic light-emitting diodes (OLEDs) are area radiative devices, and light can be efficiently emitted from a transparent electrode ITO since the refractive index of the organic materials is generally smaller than that of inorganic materials. OLEDs have a fabrication advantage in integrated circuits [3–7]; therefore, OLEDs are considered the technique of advanced flat panel display.

1.2 Ambipolar Organic Field-Effect Transistors

In 1995, Dodabalapur *et al.* achieved ambipolar transport in organic field-effect transistors (OFETs) by employing a double layer structure [8], and the mechanism was also explained by the model of separate carrier transport layers. The electrons and holes accumulate in an n-type semiconductor C_{60} layer and a p-type semiconductor α-6T layer under positive and negative gate bias, respectively (Figure 1.2). The electron and hole field-effect mobilities are about 10^{-4} cm^2/V s [8].

Introduction to Organic Semiconductor Heterojunctions Donghang Yan, Haibo Wang and Baoxun Du

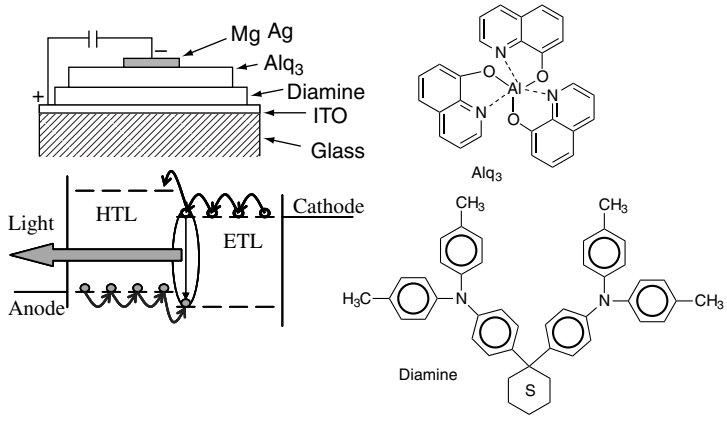

Figure 1.1 Device configuration and molecular structures. The double layer structure of diamine/Alq_3 is used as the active layer in the OLED. The diamine layer is the hole transport layer, and Alq3 layer is the electron transport and electroluminescent layer [1]. (Reprinted with permission from C.W. Tang and S.A. VanSlyke, *Applied Physics Letters*, **51**(12), 913–915, 1987. © 1987 American Institute of Physics.)

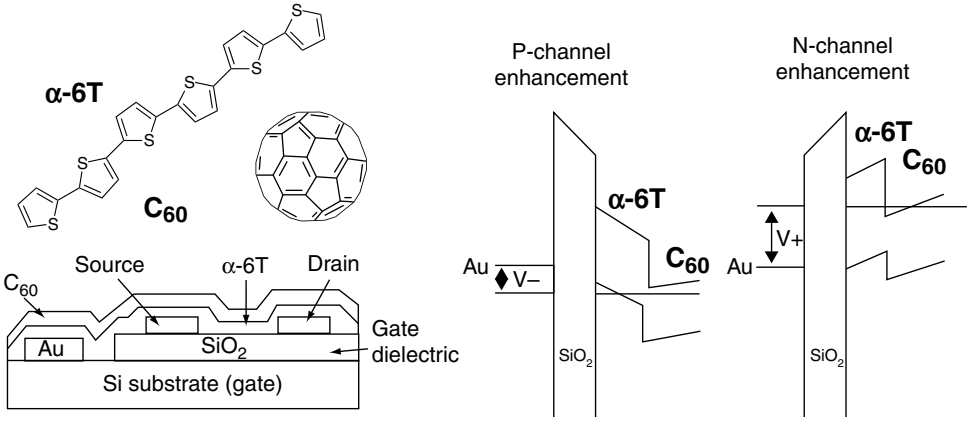

Figure 1.2 Device configuration of an ambipolar organic transistor. Electron and hole accumulation modes were realized in a single device under positive and negative gate bias, respectively [8]. (From A. Dodabalapor, H.E. Katz, L. Torsi and R.C. Haddon, "Organic heterostructure field-effect transistors," *Science*, **269**(15), 1560–1562, 1995. Reprinted with permission from AAAS.)

Ambipolar organic transistors have the advantage of a better noise margin, a lower power dissipation, and a simplified design and fabrication of ICs. Therefore, ambipolar organic transistors are promising devices in plastic radio frequency ID (RFID) tags. The RFID frequency of 13.56 MHz requires a carrier field-effect mobility over 0.1 cm^2/V s. Recently, the electron and hole mobility of organic ambipolar transistors reached 0.04 cm^2/V s, close to the target [9].

1.3 Organic Photovoltaic Cells

In 1986, C.W. Tang reported the organic photovoltaic cell (OPV) with a double layer structure as the active layer (Figure 1.3); and the power conversion efficiency reached 1%, one order of magnitude higher than Schottky cells [10, 11]. The authors think that the interface (organic heterostructure) between organic semiconductors plays a key role in the photovoltaic device.

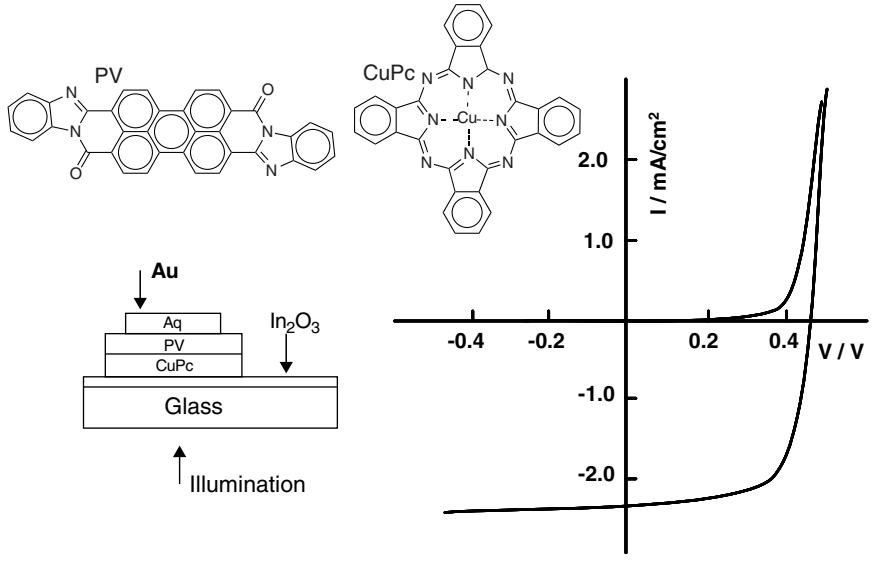

Figure 1.3 Device configuration of an organic photovoltaic cell. Photovoltage was produced between In_2O_3 and Ag, and CuPc and PV layers can transport electrons and holes, respectively [10]. (Reprinted with permission from C.W. Tang, *Applied Physics Letters*, **48**(2), 183–185, 1986. © 1986 American Institute of Physics.)

In 1995, Gang Yu reported photovoltaic cells with a MEH-PPV:C_{60} blending system [12] (Figure 1.4), and a power conversion efficiency of 2.9% was obtained under 20 mW/cm^2 and 430 nm wavelength illumination.

The blending system of MEH-PPV:C_{60} has a large donor–acceptor (D-A) area, which is called a bulk D-A heterojunction, and the scale of phase separation is at the nanometer level (Figure 1.5). Photo-generated excitons can diffuse to the D-A interface and produce free electrons and holes, consequently the efficiency is significantly improved compared with double layer OPV cells.

The scale of phase separation in a bulk heterojunction system changes with solution and annealing temperatures. Therefore, it is important to improve the efficiency by controlling the morphology and structure and by employing new crystalline materials to increase the conductivity and the absorption spectrum.

In summary, the simple energy level structure is frequently used to explain the operation process in organic electronic devices, but the details are absent. Research into the interfacial electronic structure in an organic heterojunction is of considerable importance in understanding: (i) the fundamental aspects of interface physics and (ii) the advancement of technologies for organic solid-state electronics and optoelectronics.

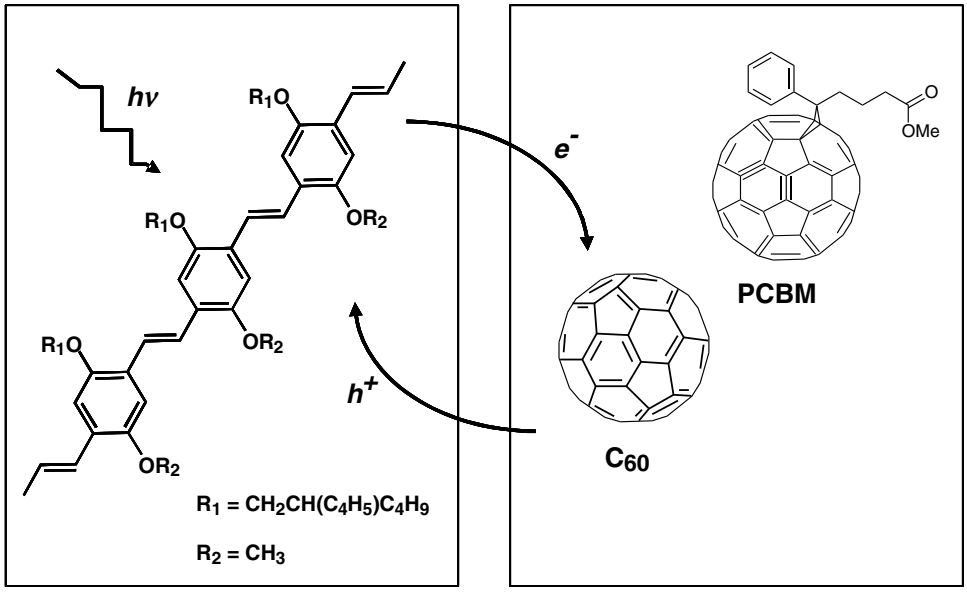

Figure 1.4 Organic photovoltaic cells of a MEH-PPV:C_{60} bulk heterojunction [12]. (From G. Yu, J. Gao, J.C. Hummelen, F. Wudl and A.J. Heeger, "Polymer photovoltaic cells: enhanced efficiencies via a network of internal donor–acceptor heterojunctions," *Science*, **270**, 1789–1791, 1995. Reprinted with permission from AAAS.)

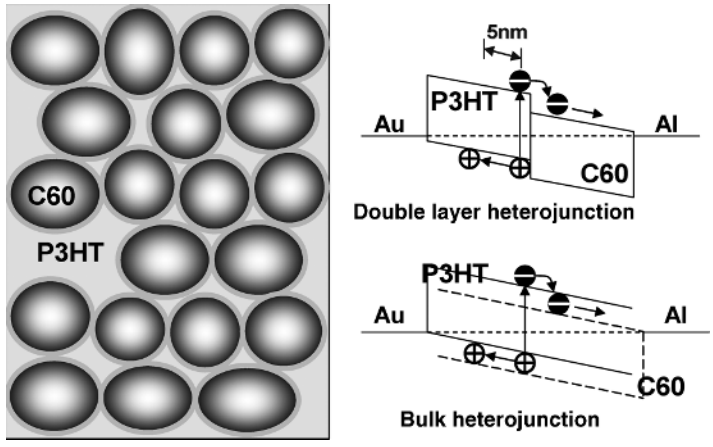

Figure 1.5 Morphostructure of a P3HT:C_{60} bulk heterojunction and the electronic structures of double layer and bulk heterojunctions.

1.4 Parameters in Thin-Film Transistors

This section introduces the output and transfer curves of organic thin-film transistors (OTFTs) and the extraction of the corresponding parameters, since some features of organic heterojunctions are characterized by OTFTs. The details of its operating process and the physical meanings of various parameters are given in the following part.

The metal–insulator–semiconductor (MIS) structure of FETs can be viewed as a parallel-plate capacitor, with the conductive gate acting as one of the capacitor plates. On the other side of the insulator, the source and drain along with the semiconductor layer (active layer) act as the other plate of the capacitor (Figure 1.6). When a gate voltage V_{GS} is applied, the carriers accumulate at the interface of the semiconductor and insulator, which increases the conductivity of organic films [13–16]. When a drain voltage V_{DS} is applied between the source and drain electrodes, the drain current I_{DS} increases, and it shows a rise with the gate voltage.

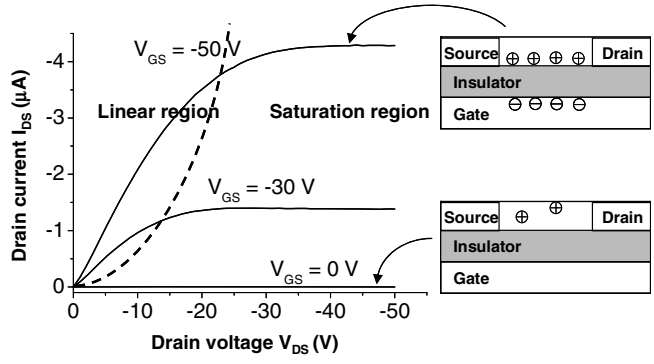

Figure 1.6 Output curve of an organic transistor operating in hole accumulation mode.

When a small V_{GS} is applied (or without V_{GS}), the carrier density in the semiconductor layer is low and consequently, the I_{DS} is small and the OTFT operates in the off state. As the V_{GS} increases, the carrier density is also increased, which leads to a high conductivity; as a result, the I_{DS} becomes large under the same V_{DS}. Therefore, OTFTs can switch between "on" and "off" under different V_{GS}, which makes it a probable logical unit in a binary system.

The carrier mobility μ and threshold voltage V_T are usually extracted from the saturation region of the transfer curve ($I_{DS} \sim V_{GS}$) according to the following equation:

$$I_{DS} = \frac{W}{2L}\mu C_i (V_{GS} - V_T)^2 \tag{1.1}$$

where C_i is the capacitance per unit area of the gate insulator and W and L are the width and length of the channel, respectively. For the curve of $I_{DS}^{1/2} \sim V_{GS}$ (Figure 1.7), its slope is proportional to the carrier mobility, and the threshold voltage V_T is the intercept from extrapolating the curve with the voltage axis. The details of OTFTs can be found in [17].

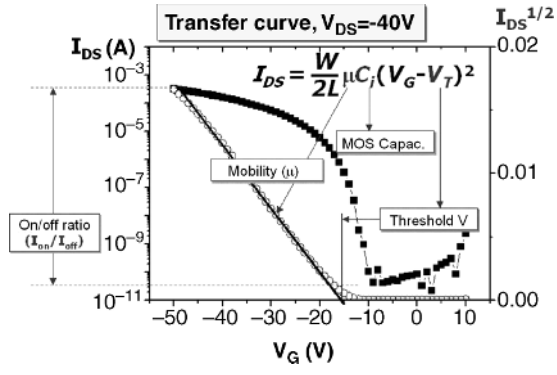

Figure 1.7 Transfer curve of an organic transistor operating in hole accumulation mode.

References

1. Tang, C.W. and VanSlyke, S.A. (1987) Organic electroluminescent diodes. *Applied Physics Letters*, **51**(12), 913–915.
2. Burroughes, J.H., Bradley, D., Brown, A.R., *et al.* (1990) Light-emitting diodes based on conjugated polymer. *Nature*, **347**, 539.
3. Cao, Y., Parker, I.D., Yu, G., *et al.* (1999) Improved quantum efficiency for electroluminescence in semiconducting polymers. *Nature*, **397**, 414–417.
4. Li, W. (2002) *Organic Electroluminescent Materials, Devices and Flat Panel Display*, Science Press, Beijing.
5. Huang, F., Hou, L.T., Wu, H.B., *et al.* (2004) High-efficiency, environment-friendly electroluminescent polymers with stable high work function metal as a cathode: green- and yellow-emitting conjugated polyfluorene polyelectrolytes and their neutral precursors. *Journal of the American Chemical Society*, **126**(31), 9845–9853.
6. Liu, J., Zhou, Q.G., Cheng, Y.X., *et al.* (2005) The first single polymer with simultaneous blue, green and red emission for white electroluminescence. *Advanced Materials*, **17**(24), 2974–2978.
7. Huang, C.H., Li, F.Y., and Huang, W. (2005) *Introduction to Organic Electroluminescent Materials and Devices*, Fudan Press, Shanghai.
8. Dodabalapur, A., Katz, H.E., Torsi, L., and Haddon, R.C. (1995) Organic heterostructure field-effect transistors. *Science*, **269**(5230), 1560–1562.
9. Klauk, H. (2006) *Organic Electronics: Materials, Manufacturing, and Applications*, Wiley-VCH Verlag GmbH & Co. KGaA, Weinheim.
10. Tang, C.W. (1986) Bi-layer organic photovoltaic cell. *Applied Physics Letters*, **48**(2), 183–185.
11. Sariciftci, N.S., Smilowitz, L., Heeger, A.J., and Wudl, F. (1992) Photoinduced electron transfer from a conducting polymer to buckminsterfullerene. *Science*, **258**, 1474–1476.
12. Yu, G., Gao, J., Hummelen, J.C. *et al.* (1995) Polymer photovoltaic cells: Enhanced efficiencies via a network of internal donor–acceptor heterojunctions. *Science*, **270**, 1789–1791.
13. Brabec, C.J., Sariciftci, N.S., and Hummelen, J.C. (2001) Plastic solar cells. *Advanced Functional Materials*, **11**(1), 15–26.
14. Peumans, P., Yakimov, A., and Forrest, S.R. (2003) Small molecular weight organic thin-film photodetectors and solar cells. *Journal of Applied Physics*, **93**(7), 3693–3723.
15. Hoppe, H. and Saricftci, N.S. (2004) Organic solar cells: An overview. *Journal of Materials Research*, **19**(7), 1924–1945.
16. Brütting, W. (2005) *Physics of Organic Semiconductors*, Wiley-VCH Verlag GmbH & Co. KGaA, Weinheim.
17. IEEE (2004) Std 1620-2004. *IEEE Standard Test Methods for the Characterization of Organic Transistors and Materials*, IEEE.